Cell

The WAVE Regulatory Complex Links Diverse Receptors to the Actin Cytoskeleton

Baoyu Chen,[1] Klaus Brinkmann,[2,3] Zhucheng Chen,[1,3,4] Chi W. Pak,[1,3] Yuxing Liao,[1] Shuoyong Shi,[1] Lisa Henry,[1] Nick V. Grishin,[1] Sven Bogdan,[2,*] and Michael K. Rosen[1,*]

[1]Department of Biophysics and Howard Hughes Medical Institute, University of Texas Southwestern Medical Center at Dallas, 5323 Harry Hines Boulevard, Dallas, TX 75390, USA

[2]Institut für Neurobiologie, Universität Münster, 48149 Münster, Germany

[3]These authors contributed equally to this work and are listed in alphabetical order

[4]Present address: School of Life Sciences, Tsinghua University, Beijing 100084, China

*Correspondence: sbogdan@uni-muenster.de (S.B.), michael.rosen@utsouthwestern.edu (M.K.R.)

http://dx.doi.org/10.1016/j.cell.2013.11.048

SUMMARY

The WAVE regulatory complex (WRC) controls actin cytoskeletal dynamics throughout the cell by stimulating the actin-nucleating activity of the Arp2/3 complex at distinct membrane sites. However, the factors that recruit the WRC to specific locations remain poorly understood. Here, we have identified a large family of potential WRC ligands, consisting of ~120 diverse membrane proteins, including protocadherins, ROBOs, netrin receptors, neuroligins, GPCRs, and channels. Structural, biochemical, and cellular studies reveal that a sequence motif that defines these ligands binds to a highly conserved interaction surface of the WRC formed by the Sra and Abi subunits. Mutating this binding surface in flies resulted in defects in actin cytoskeletal organization and egg morphology during oogenesis, leading to female sterility. Our findings directly link diverse membrane proteins to the WRC and actin cytoskeleton and have broad physiological and pathological ramifications in metazoans.

INTRODUCTION

The actin cytoskeleton undergoes highly dynamic rearrangements, a process that is vital to all eukaryotic cells. Members of the Wiskott-Aldrich syndrome protein (WASP) family are ubiquitous regulators of actin cytoskeletal dynamics (Campellone and Welch, 2010; Padrick and Rosen, 2010). WASP proteins are defined by a conserved C-terminal VCA (Verprolin-homology, Central, Acidic) sequence that stimulates the actin-nucleating activity of the Arp2/3 complex. The WASP family verprolin homologous protein (WAVE) is found in all eukaryotic kingdoms and plays a central role in many cellular processes, including adhesion, migration, division, and fusion (Pollitt and Insall, 2009; Takenawa and Suetsugu, 2007). In animals, WAVE proteins play diverse roles ranging from embryogenesis, neuron morphogenesis and plasticity, immune cell activation and chemotaxis, to cancer invasion and metastasis (Pollitt and Insall, 2009; Takenawa and Suetsugu, 2007).

In cells, WAVE is constitutively incorporated into a conserved, heteropentameric complex of ~400 kDa named the WAVE regulatory complex (WRC). This complex consists of the following five components: Sra1/Cyfip1 (or the ortholog PIR121/Cyfip2), Nap1/Hem2/Kette (or the ortholog Hem1), Abi2 (or the orthologs Abi1 and Abi3), HSPC300/Brick1, and WAVE1/SCAR (or the orthologs WAVE2 and WAVE3) (Eden et al., 2002). Different WRC isoforms can be assembled from combinations of different orthologs of each component (Takenawa and Suetsugu, 2007). The structure of the WRC revealed that the complex can be viewed as two subcomplexes: a dimer formed by pseudosymmetric association of the two large, homologous proteins Sra1 and Nap1 and a trimer formed by the N terminus of WAVE1, Abi2, and HSPC300 forming a four-helix bundle (Figure 1A) (Chen et al., 2010). Within the WRC, the activity of WAVE toward the Arp2/3 complex is inhibited by intracomplex sequestration of its VCA (Chen et al., 2010). In response to upstream signals, the WRC is both recruited to the membrane and triggered to release its inhibition of WAVE, which are cooperative events that are required to achieve optimal activity (Lebensohn and Kirschner, 2009; Padrick et al., 2008; Padrick and Rosen, 2010; Suetsugu et al., 2006).

Many WRC ligands have been described and mainly fall into four distinct classes based on their mechanism of interaction. The first consists of small GTPases: Rac directly binds to Sra1 and activates the WRC by allosterically releasing the bound VCA (Chen et al., 2010), and Arf can act cooperatively with Rac to promote WRC activation at membranes (Koronakis et al., 2011). The second consists of acidic phospholipids (phosphatidylinositol (3,4,5)-trisphosphate, PIP_3, and perhaps others), which enhance WRC association with membranes likely via electrostatic interactions (Oikawa et al., 2004). The third class contains various kinases, including Abl, Cdk5, and ERK2, which phosphorylate the WRC and may regulate its activity by destabilizing VCA sequestration or modulating its interactions with other

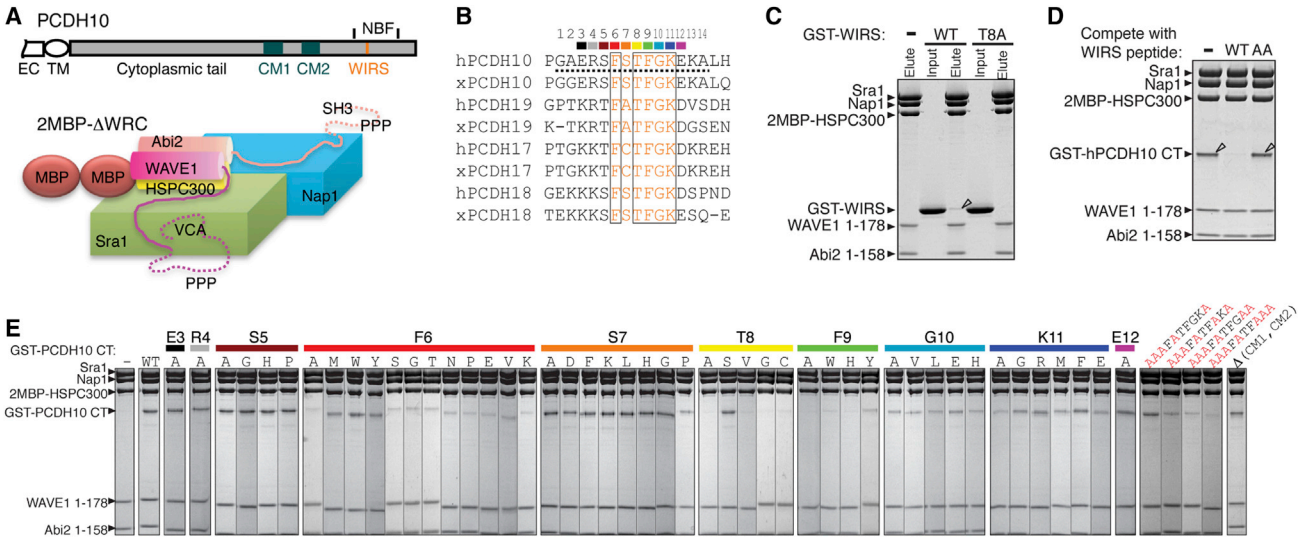

Figure 1. PCDH10 CT Binds to the WRC Using WIRS

(A) Schematic representation of PCDH10 (extracellular domain cropped) and the WRC.

(B) Sequence alignment of PCDH10-homologous protocadherin tails (h, human; x:, *Xenopus tropicalis*; dashed line indicates peptide used in crystallography). WIRS is orange, and conserved residues are in black boxes. Residues mutated in (E) are color coded.

(C–E) Coomassie-blue-stained SDS-PAGE gels show that immobilized 2MBP-ΔWRC selectively retained GST-WIRS peptide (C), GST-hPCDH10 CT (879-1014) (D), or GST-mPCDH10 CT (778-1014) (E). Triangles indicate bound proteins. In (D), the WIRS peptide, but not a mutant (AA for T8A/F9A), blocked this interaction. In (E), amino acid substitutions are shown below the color-coded WT residues or in red letters.

See also Figure S1.

proteins (Takenawa and Suetsugu, 2007). The fourth class contains multimodule scaffolding proteins, including IRSp53, Toca1, and WRP, which often utilize SH3 domains to interact with the proline-rich regions of Abi2 and WAVE1 and likely facilitate membrane recruitment and clustering of the WRC (Lebensohn and Kirschner, 2009; Padrick et al., 2008; Padrick and Rosen, 2010; Takenawa and Suetsugu, 2007).

More recently, two single-pass transmembrane cell-adhesion proteins, protocadherin 10 (PCDH10) and PCDH19, were reported to interact with the WRC (Nakao et al., 2008; Tai et al., 2010). These proteins do not belong to any of the four known classes of WRC ligands; therefore, we wondered whether they might represent a new class. Moreover, PCDH10 and PCDH19 are important to brain development (Emond et al., 2009; Uemura et al., 2007) and are implicated in autism, epilepsy, and mental retardation (Dibbens et al., 2008; Morrow et al., 2008). PCDH10 also functions as a tumor suppressor in many cancers (Ying et al., 2006). However, little is known about how these proteins—or the protocadherin family in general—signal downstream. A detailed characterization of interactions of PCDH10/19 with the WRC and the actin cytoskeleton might provide valuable clues to the functions of these proteins and their many relatives in the protocadherin family.

Here, through further biochemical studies of the PCDH10/WRC interaction, we have identified a conserved peptide motif, the WRC interacting receptor sequence (WIRS), that directly binds a conserved surface on the WRC both in vitro and in cells. We further identified ~120 diverse transmembrane or membrane associated proteins that contain the WIRS motif, including protocadherins, ROBO proteins, netrin receptors, neuroligins, G-protein-coupled receptors (GPCRs), and ion channels, among others. Disrupting the WIRS-binding surface of the WRC in flies causes defects in actin organization and egg morphology during oogenesis, leading to female sterility, and also causes defects in optic lobe development. Together, our biochemical, structural, cellular, and genetic data reveal a highly conserved and widespread interaction motif that links diverse membrane proteins to the WRC and the actin cytoskeleton.

RESULTS

The WRC Binds to a Conserved Peptide Motif in the Cytoplasmic Tail of PCDH10

The initial reports describing an interaction between PCDH10 or PCDH19 and the WRC left two important questions unanswered: (1) whether the interaction was direct and (2) which sequence(s) were responsible (Nakao et al., 2008; Tai et al., 2010). To begin addressing the first question, we assembled recombinant WRC containing HSPC300 with two maltose-binding proteins (MBPs) fused in tandem to its N terminus (2MBP-ΔWRC, Figure 1A). Immobilized 2MBP-ΔWRC efficiently retained the purified cytoplasmic tail (CT) of PCDH10 (Figures 1D and 1E). The PCDH10 tail and 2MBP-ΔWRC also coeluted during gel filtration chromatography (Figure S1A). Finally, isothermal titration calorimetry (ITC) indicated 1:1 binding stoichiometry with a dissociation equilibrium constant (Kd) of 0.3 μM (Figure S1B). These data indicate that PCDH10 CT directly binds the WRC.

We next addressed the second question: which sequence(s) are responsible for the interaction? Previous studies of

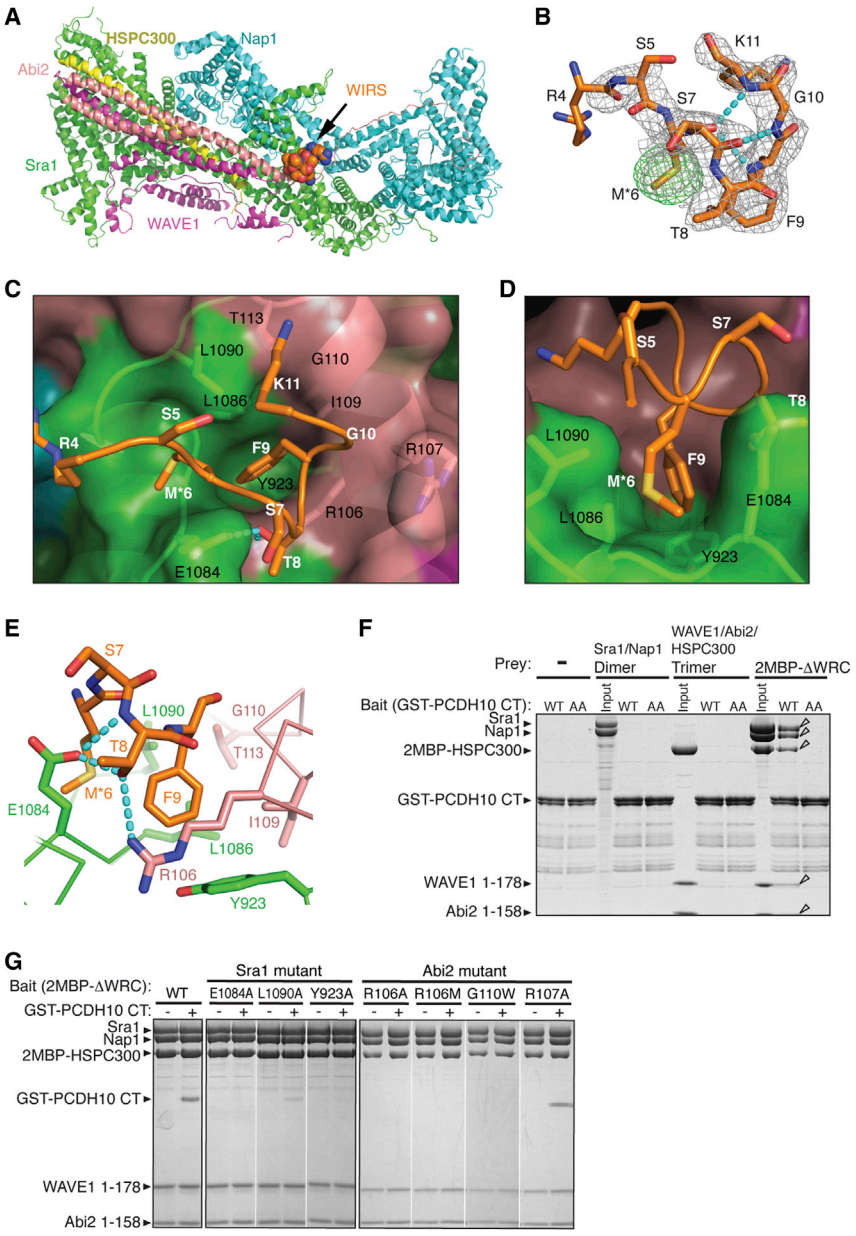

Figure 2. WIRS Binds to a Composite Surface Formed by Sra1 and Abi2

(A) Structure of the WIRS/WRC complex (Sra1, green; Nap1, cyan; HSPC300, yellow; Abi2, pink; WAVE1, magenta; and WIRS peptide, spheres).

(B) 2Fo-Fc electron density map (gray mesh, 1.2 σ) and anomalous scattering map (green mesh, 4 σ) around the WIRS peptide. Cyan dotted lines show intrapeptide hydrogen bonds.

(C and D) Top and side views of a semitransparent WRC surface (key side chains shown under the surface, black labels) with WIRS peptide (white labels).

(E) WRC-WIRS interactions; dotted lines show intermolecular hydrogen bonds.

(F and G) Coomassie-blue-stained SDS-PAGE gels of eluted proteins are shown. In (F), immobilized GST-PCDH10 CT WT or mutant (AA for T1002A/F1003A) selectively retained WRC, but not indicated subcomplexes. Open triangles indicate bound proteins. In (G), immobilized 2MBP-ΔWRC mutants selectively retained GST-PCDH10 CT.

See also Figure S2 and Table S1.

PCDH10 and PCDH19 suggested two candidate elements: (1) the CM2 (conserved motif 2) sequence, conserved throughout the δ-protocadherin family to which both protocadherins belong, and (2) a more C-terminal region of the tail named the Nap1-binding fragment (NBF), proposed to interact with the Nap1 subunit of the WRC (Figure 1A) (Nakao et al., 2008). We found that the CM2 motif is not required for direct binding (Figure 1E). Instead, our sequence alignment of the δ-protocadherins most closely related to PCDH10 revealed a conserved nine residue sequence, RSFSTFGKE, within the NBF element (Figure 1B). A peptide containing this sequence directly bound the WRC and blocked the interaction with PCDH10 CT (Figures 1C and 1D). The interaction was specifically abolished by mutation of the conserved threonine to alanine (Figures 1C and 1D). Thus, we conclude that this sequence is both necessary and sufficient for binding the WRC. We then systematically introduced point mutations to the PCDH10 CT throughout this conserved sequence and measured binding of the mutant proteins to the WRC. The results identified a weak six residue consensus motif, Φ-x-T/S-F-X-X (Φ = preference for bulky hydrophobic residues; x = any residue; the X-X positions can accommodate single substitutions, but not all combinations of double substitutions, Figure 1E). We named this new motif WIRS (Figure 1E).

Crystal Structure of the WIRS/WRC Complex Reveals Binding Mechanism

We next sought to determine where and how the WIRS motif binds to the WRC. For this, we determined the 2.43-Å crystal structure of a complex cocrystallized from a variant of the WIRS-containing peptide (WGAERSM*STFGKEKA, M* for selenomethionine, Figure 1B) and a minimal inhibited WRC, which lacks the C terminus of Abi and the proline-rich region of WAVE, miniWRC (Figure 2 and Table S1) (Chen et al., 2010). We observed electron density for eight residues of the bound WIRS peptide (Figure 2B) and assigned the sequence unambiguously to RSM*STFGK, assisted by anomalous dispersion from the selenomethionine (M*), which allowed us to resolve the pseudo-2-fold symmetry of the peptide about the ST sequence (Figure 2B).

The overall structure of the complex reveals several notable features of the interaction. First, the overall structure of the

peptide-bound miniWRC, including the VCA region of WAVE1, is nearly identical to that of the apo form (Chen et al., 2010) with backbone root-mean-square deviation (rmsd) of 0.3 Å (Figure S2). This near identity suggests that WIRS binding per se may not activate the WRC (see also below). Second, the STFG sequence forms a type-I β-turn, which contains a stereotypical backbone hydrogen bond between the S7 carbonyl and G10 amide and additional backbone hydrogen bonds from the M*6 carbonyl to the F9 and K11 amides (Figure 2B). Third, the WIRS binds to a composite surface of the WRC, which is formed by both Sra1 and Abi2 (Figures 2A, 2C, and 2D). Because Sra1 is part of the large Sra1/Nap1 subcomplex and Abi2 is part of the Abi2/WAVE1/HSPC300 subcomplex, as suggested by topology of the WRC structure and biochemical reconstitution, Sra1 and Abi2 come together only when the WRC is assembled from these subcomplexes (Chen et al., 2010; Ismail et al., 2009). This means that the WIRS binds only to the fully assembled WRC. In agreement, the PCDH10 CT cannot bind WRC subcomplexes containing only Sra1 or Abi2 (Figure 2F). Fourth, in contrast to previous suggestions based on immunoprecipitation data (Nakao et al., 2008), no contacts are observed between the peptide and Nap1.

Finally, the structure of the WIRS binding surface clearly explains the specificity of the consensus WIRS motif, Φ-x-T/S-F-X-X, derived from the biochemical assays above. M*6 (the Φ1 position) packs against E1084 and L1090 of Sra1 and F9 of the WIRS. It acts as a "plug" that completes a deep hydrophobic pocket that binds F9, as described below (Figure 2D), explaining the preference for large hydrophobic residues at the Φ1 position. The side chain of S7 (the x2 position) is directed toward solvent and can be readily altered without affecting binding (Figure 2D). The side chain of T8 (the T/S3 position) forms a network of hydrogen bonds bridging E1084 of Sra1 and R106 of Abi2, with E1084 forming another hydrogen bond with the T8 amide (Figure 2E). This network explains why only threonine and serine are tolerated at the third position in the WIRS sequence. The side chain of F9 (the F4 position) inserts into a deep and narrow hydrophobic pocket formed by Y923, E1084, L1086, and L1090 of Sra1 and R106, I109, G110, and T113 of Abi2 and is completed by M*6 from the WIRS peptide (Figures 2C and 2E). The aromatic ring of F9 stacks against that of Y923 of Sra1 and makes cation-π interactions with R106 of Abi2 (Figure 2E). Together, these explain why phenylalanine is strongly preferred at this position (with tyrosine affording observable, but weaker binding; Figure 1E). G10 and K11 (the last X-X positions) do not contact the WRC, allowing many residues at these positions (data not shown). G10 adopts a left-handed conformation in order to position K11 to hydrogen bond with M*6. As this conformation is energetically favorable only for glycine, it is likely that other amino acids at position 10 would adopt different conformations, and the K11/M*6 hydrogen bond may not be generally observed. In support of the observed interactions, point mutations to the contact residues on either Sra1 (E1084A, L1090A, or Y923A) or Abi2 (R106A, R106M, or G110W) all abolished binding to the PCDH10 CT (Figures 2C and 2G). In contrast, changing a proximal residue (Abi2 R107A) that does not contact WIRS had no effect (Figures 2C and 2G).

The WIRS Binding Surface Is Highly Conserved in Metazoans

The WIRS binding surface is nearly 100% conserved in metazoans, spanning from human to sponge, including all isoforms of Sra and Abi (Figure 3). This strongly suggests that WIRS/WRC interactions in general are vital to all animals. Indeed, purified *Drosophila* WRC (2MBP-dWRC) also bound to the wild-type (WT) human PCDH10 CT, but not the mutant with a disrupted WIRS (Figure 3D). Disrupting the binding surface on the *Drosophila* WRC (2MBP-dWRC$_{AW}$, containing an Abi equivalent to human R106A/G110W) also abolished the interaction (Figure 3D). Only a few such conserved surface patches exist on the WRC (Figure 3C), including the Rac GTPase binding site on the opposite side of the complex (data not shown) (Chen et al., 2010). The WIRS binding site is conserved even in the WRCs of nonmetazoan choanoflagellates, but not in other WRC-expressing nonmetazoans, including protists, fungi, and plants (Figures 3A and 3B). Choanoflagellates are considered to be the closest unicellular relatives to metazoans (King et al., 2008), and some species have a multicellular stage in their life cycle (Alegado et al., 2012). The only metazoan in which the WIRS binding surface is not conserved is the placozoan *Trichoplax adhaerens*, which is arguably the simplest free-living animal whose phylogenetic classification remains controversial (Srivastava et al., 2008).

Many Membrane Proteins Contain a WIRS in Their Cytoplasmic Regions

We next searched the Swiss-Prot database (Lane et al., 2012) to find other human proteins that might use WIRS motifs to bind the WRC. Given the relatively low sequence complexity of the WIRS motif itself, we limited the search to proteins resembling PCDH10—membrane or membrane-associated proteins in which the motif is flanked by disordered sequences and thus not part of a folded domain. We further used sequence conservation as another criterion to increase our search stringency—we removed ligands whose WIRS motifs were found in less than four of the seven species: human, mouse, chicken, frog, zebrafish, *Drosophila*, and *C. elegans*. Although these restrictions may exclude some potential ligands, they should limit false positives (Figure 4).

Using these criteria, we obtained 115 potential WIRS-containing WRC ligands (Table S2; see http://prodata.swmed.edu/WIRS/ for unfiltered results). Most of these are cell-cell adhesion proteins or receptors, but some are ion channels or scaffolding proteins. They include 15 members of the protocadherin-α family (PCDHα), 9 other protocadherins, 4 neuroligins, 2 ROBO receptors, 3 netrin receptors, various GPCRs, and several ion channels. Many of these proteins are enriched in the nervous or immune systems, although others are widely expressed (Table S2). Of these, only five, including PCDH10, PCDH19, the netrin receptor DCC (Bernadskaya et al., 2012; Stavoe et al., 2012), the Slit receptor ROBO1 (Bernadskaya et al., 2012), and the epithelial Na(+) channel ENaC (Karpushev et al., 2011), have been previously shown to interact with the WRC biochemically or genetically. Furthermore, only a small number have been previously connected with the actin cytoskeleton (Figure 4 and Table S2).

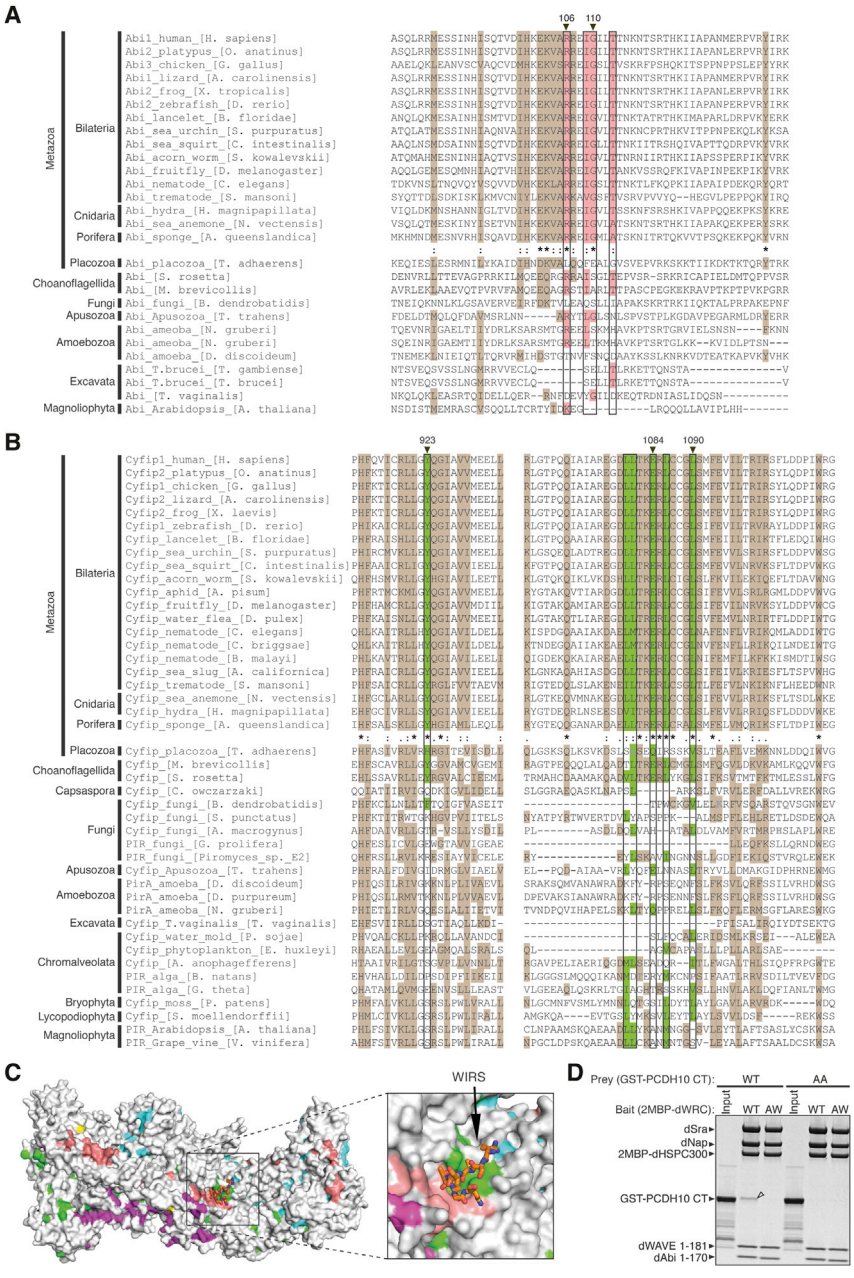

Figure 3. WIRS Binding Surface Is Highly Conserved

(A and B) Sequence alignments of representative organisms. Surface residues of the WIRS binding site (black boxes) are highlighted with pink for Abi (A) and green for Sra (B). Other conserved residues were highlighted with brown. Degrees of conservation up to Porifera are represented with ClustalW symbols (asterisk [*] for no change, colon [:] for conserved, and period [.] for less conserved changes). Residues whose mutation disrupts WIRS binding in Figure 2 are labeled with black triangles on top. Gray amino acids indicate where sequence insertions in alignment were not shown.

(C) Surface conservation of the WRC, with the most conserved surface residues (ConSurf score 9) (Ashkenazy et al., 2010) colored as in Figure 2A and less conserved residues (ConSurf score < 9) colored in gray.

(D) Coomassie-blue-stained SDS-PAGE gel shows that immobilized WT *Drosophila* WRC, but not a mutant with a disrupted WIRS binding surface (AW for R118A/G122W-dAbi), selectively retained GST-PCDH10 CT (WT), but not a mutant (AA for T1002A/F1003A).

WIRS-Containing Tails Have Various Effects on WRC Activity

To understand the function of the WIRS/WRC interaction, we first tested whether the cytoplasmic tail of PCDH10 (PCDH10 CT) could activate the WRC in Arp2/3-mediated pyrene-actin assembly assays. Based on our crystal structure of the WIRS-bound WRC in which the VCA of WAVE1 remains sequestered and inhibited by Sra1, we anticipated that PCDH10 or, more precisely, WIRS binding would not be sufficient to activate the WRC. As anticipated, neither the WIRS peptide nor the PCDH10 CT increased activity of the WRC toward the Arp2/3 complex (Figures 5A and 5B). Somewhat unexpectedly, however, in the presence of subsaturating concentrations of Rac1, PCDH10 CT enhanced the ability of Rac1 to stimulate WRC activity (Figure 5B), suggesting that the two ligands can act cooperatively. When the WRC was saturated by higher concentrations of Rac1, PCDH10 CT could not enhance activity further (Figure 5B). These data suggest that PCDH10 CT may act by modestly shifting the autoinhibitory equilibrium of the WRC. Such a shift could facilitate activation by Rac1 while providing only minimal (below measurement threshold) activation on its own (Buck et al., 2004). This cooperative activation is reminiscent of the coactivation of the WAVE relative, N-WASP, by Toca1 and the GTPase Cdc42 (Ho et al., 2004). Notably, the minimal WIRS peptide had no effect on Rac1 stimulation, indicating that flanking sequences in the PCDH10 CT are needed for this activity (Figure 5A).

To verify our search results, we purified GST-fused cytoplasmic tails of 18 of these potential ligands and examined their interactions with the WRC using pull-down assays. We found that 13 of these tails, including Neuroligin-1, Neuroligin-4X, ROBO1, Cav1.3, LRIG3, PCDH8, PCDH10, PCDH12, PCDH17, PCDH18, PCDH19, PCDHα6, and FAT3, bound the WT WRC, but not a mutant whose WIRS-binding surface was disrupted by mutations (2MBP-ΔWRC$_{AW}$, containing R106A/G110W-Abi2; Figure 4). Disrupting the WIRS binding surface did not affect WRC binding to Rac1, suggesting that the point mutations only locally disrupted the WIRS-binding site. Therefore, we have identified a large and diverse class of WRC ligands.

A

Protein	WIRS	Function	Actin	Disease
Neuroligin-1	PLHTFNTFTGGQNN	Adhesion	yes	Autism
Neuroligin-4X	PLHTFNTFSGGQNS	Adhesion	n.a.	Autism; Mental retardation; Tourette syndrome
ROBO1	KINEMKTFNSPNLK	Receptor	yes	Dyslexia; Schizophrenia; AMD; Cancer
Cav1.3	PDISYRTFTPASLT	Channel	n.a.	SANDD syndrome
LRIG3	SNSFMGTFGKALRR	n.a.	n.a.	Cancer
PCDH8	PPAQMSTFCKSTSL	Adhesion	n.a.	Cancer
PCDH10	DRCWMPSFVPSDGR	Adhesion	yes	Autism; Cancer
	AERSFSTFGKEKAL			
PCDH12	EPRTFQTFGKAEAP	Adhesion	n.a.	Schizophrenia
PCDH17	GKKTFCTFGKDKRE	Adhesion	n.a.	Cancer
PCDH18	KKKSFSTFGKDSPN	Adhesion	n.a.	Intellectual disability
PCDH19	TKRTFATFGKDVSD	Adhesion	n.a.	Epilepsy in females with mental retardation; Dravet syndrome
PCDHα6	DKSDFITFGKKEET	Adhesion	yes	Bipolar disorder; Cancer
FAT3	EHQEMTTFHPESPR	Adhesion	n.a.	n.a.
	EVQSLSSFQSDSGD			

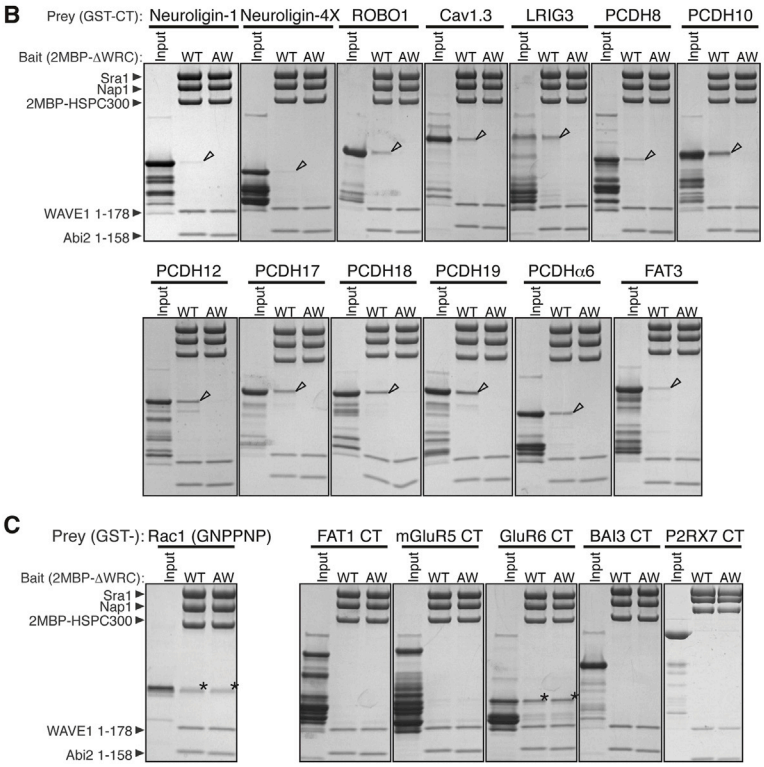

Figure 4. Many WIRS Proteins Bind the WRC

(A) WIRS ligands that bind WRC in pull-down assays with WIRS highlighted in orange. See Table S2 for references.

(B and C) Coomassie-blue-stained gels show proteins selectively retained by immobilized 2MBP-ΔWRC (WT for wild-type, AW for R106A/G110W-Abi2). (B) shows verified cytoplasmic tails of WIRS proteins, and (C) shows false positive WIRS ligands. Arrows denote bound proteins. Asterisks indicate protein bound to the WRC independent of the WIRS interaction. GST-Rac1-GMPPNP is a positive control.

See also Table S2.

We further tested seven additional cytoplasmic tails from the above-verified WIRS proteins (Figure 5C) and found that they have different effects on activity of the WRC. The tails of PCDH19 and PCDH12 were able to enhance Rac1-mediated WRC activation, similar to that of PCDH10. The tails of the other proteins either had no effect on activity or were slightly inhibitory. These data suggest that the activity of WIRS ligands is variable, with some merely binding the WRC and others further modulating its activity.

WIRS Ligands Bind the WRC In Vivo

Having shown that WIRS proteins directly bind to the WRC using purified recombinant proteins, we tested whether this interaction also occurred between endogenous proteins. We found that recombinant GST-PCDH10 CT can pull down endogenous WRC from mouse brain lysate (Figure 6A), which is consistent with previous results (Nakao et al., 2008). Addition of the WT WIRS peptide (WIRS WT) in this reaction completely blocked the interaction, whereas the peptide with a disrupted WIRS motif (WIRS AA) had no effect. Further, an antibody targeting the acidic region of the WAVE1 VCA could coimmunoprecipitate WRC and full-length PCDH10 from mouse brain lysate (Figure 6B). As above, this interaction was weakened by the WIRS WT peptide but, to a lesser extent, by the mutant WIRS AA peptide (Figure 6B). Thus, consistent with our in vitro results using recombinant proteins, the interaction between endogenous PCDH10 and endogenous WRC is WIRS dependent.

We next examined whether PCDH10 could specifically recruit the WRC to the plasma membrane in cells. We engineered a chimeric transmembrane receptor composed of the extracellular domain of CD16, the transmembrane domain of CD7, the cytoplasmic tail of PCDH10, and a C-terminal mCherry tag (CD16-CD7-PCDH10 CT-mCherry) (Kolanus et al., 1993). This chimeric receptor was expressed in NIH 3T3 cells also stably expressing Sra1-YFP. Dynal beads coated with anti-CD16 antibodies were then added to cluster the receptors at discrete regions where the beads contact the cells. Confocal images of beads that successfully recruited and clustered the chimeric receptors showed enrichment of mCherry tag (Figure 6C, red channel). At the same receptor-enriched regions, we observed significantly greater corecruitment of the WRC (Figure 6C, green channel) for the wild-type receptor tail than for the mutant tail in which the WIRS motif was disrupted (Figures 6C and 6D). This is consistent with the previous observations by Nakao et al. (2008) that PCDH10 recruits the WRC to cell-cell contact sites. We also examined two other proteins using the same assay, PCDH17 and Neuroligin1. The PCDH17 tail, which

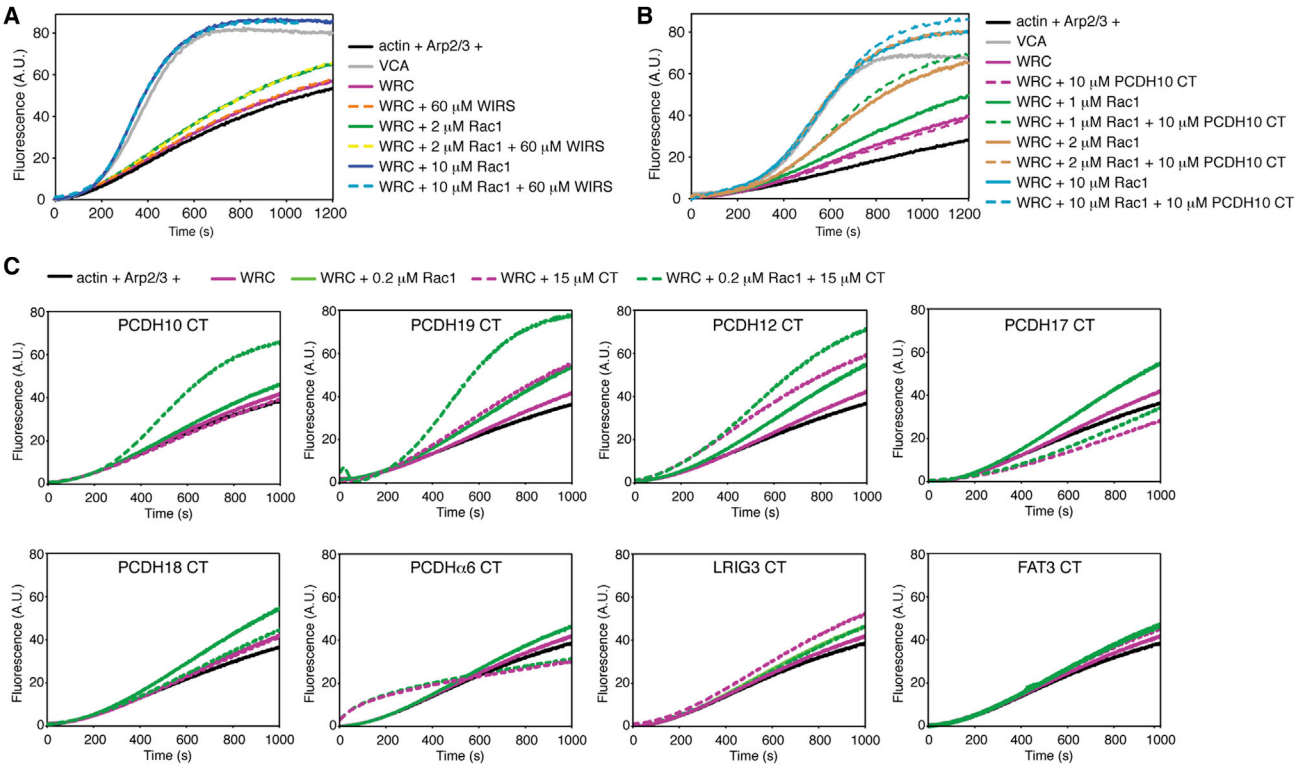

Figure 5. WIRS-Containing Tails Have Various Effects on WRC's Activity

(A–C) Actin assembly assays of WIRS (A), PCDH10 CT (B), or other WIRS-containing tails (C). Reactions contain 4 μM actin (5% pyrene labeled), 10 nM Arp2/3 complex, 100 nM WRC217 or VCA (A and B), 50 nM FL-WRC (C), and/or Rac1 where indicated.

binds the WRC with similar affinity as the PCDH10 tail (Figure S3), exhibited similar WIRS-dependent recruitment of the WRC (Figure 6D). The Neuroligin-1 tail, which binds the WRC ~20 fold more weakly than PCDH10 (Figure S3), also recruited the assembly but with less statistical certainty ($p = 0.10$, Figure 6D). Thus, we posit that WIRS ligands are sufficient and necessary to recruit the WRC in cells.

Mutating the WIRS-Binding Surface Disrupts Oogenesis in Flies

To explore the physiologic functions of the WIRS/WRC interaction, we used *Drosophila* oogenesis as a model system and investigated the consequences of disrupting the WIRS binding site of the WRC. Previous studies had revealed that normal oogenesis in *Drosophila* depends on the functions of the WRC and the Arp2/3 complex (Zallen et al., 2002). During oogenesis, *Drosophila* ovaries produce egg chambers, which progressively mature through 14 morphologically distinct stages to become eggs competent for fertilization (Bastock and St Johnston, 2008; Bilder and Haigo, 2012; Hudson and Cooley, 2002b). An egg chamber is mainly occupied by one oocyte and 15 nurse cells interconnected by actin-rich cytoplasmic bridges termed ring canals. The nurse cells provide nutrients and macromolecules for the oocyte through the ring canals. At the end of stage 10, the nurse cells start to contract and squeeze the cytoplasmic contents into the oocyte, a process termed "dumping," which requires cytoplasmic actin bundles to form a basket-like structure that prevents nuclei from clogging the ring canals. Disruption of this "dumping" process results in female sterility as previously shown for *wave* and *arp2/3* complex mutants (Hudson and Cooley, 2002a; Zallen et al., 2002). We recently reported similar results of female sterility in zygotically rescued *abi* mutant flies, which also displayed a characteristic dumpless egg mutant phenotype (Zobel and Bogdan, 2013).

To determine whether the WIRS-binding surface of the WRC (and thus potentially a WIRS/WRC interaction) plays a role during this process, we attempted to rescue normal oogenesis and female fertility by generating transgenic flies that re-expressed Abi WT or a mutant with a disrupted WIRS binding surface (dAbi-AW) in an *abi* mutant background using site-specific ΦC31-mediated integration (Bischof et al., 2007). To drive efficient expression in the maternal germline, we specifically generated pUASp transgenes (Rørth, 1998). We found that ubiquitous re-expression (*da*-Gal4) of dAbi-AW rescued the dumpless egg phenotype and female sterility (as shown by reduction of offspring number) with significantly less efficiency than did re-expression of dAbi-WT (Figures 7A and 7B). The incomplete rescue by dAbi-WT was likely due to the weak maternal expression of ubiquitous *da*-Gal4 driver (Rørth, 1998) (Figures 7A and 7B).

To understand why the dAbi-AW rescued eggs were defective, we examined maturing egg chambers and found obvious

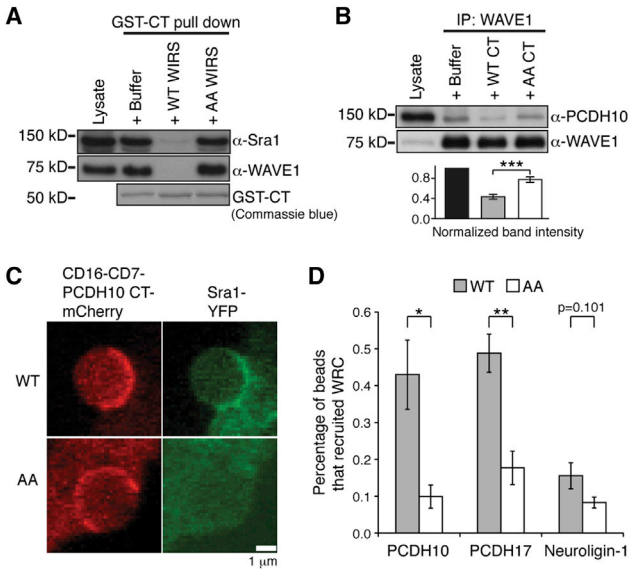

Figure 6. WIRS Proteins Bind the WRC in Cells

(A) Western blots show endogenous WRC retained from mouse brain lysate by immobilized GST-PCDH10 CT, competed by buffer or 100 μM WIRS peptides (WT for wild-type, AA for T8A/F9A).

(B) Coimmunoprecipitation of WAVE1 from mouse brain lysate, competed by buffer or 500 μM GST-PCDH10 CT (WT for wild-type, AA for T1002A/F1003A; similar results achieved by 5 mM WIRS peptide, see also Extended Experimental Procedures). Quantification of immunoprecipitated PCDH10 is shown below the corresponding samples (n = 7, p = 0.00003, including experiments competed with GST-PCDH10 CT or WIRS peptides).

(C) Representative confocal images showing antibody-coated beads clustering mCherry-tagged chimeric CD16-CD7-PCDH10 CT receptor (red) expressed in NIH 3T3 cells stably expressing Sra1-YPet (green).

(D) Quantification of images represented in (C) for tails of PCDH10 (n = 6, p = 0.014), PCDH17 (n = 4, p = 0.0045), and Neuroligin1 (n = 6, p = 0.10). Each repeat (n) used ~40 or 20 total beads for the WT and mutant tails, respectively. Error bars represent SEM, and p values were calculated by Student's t test (*p < 0.05, **p < 0.005, and ***p < 0.0005). See also Figure S3.

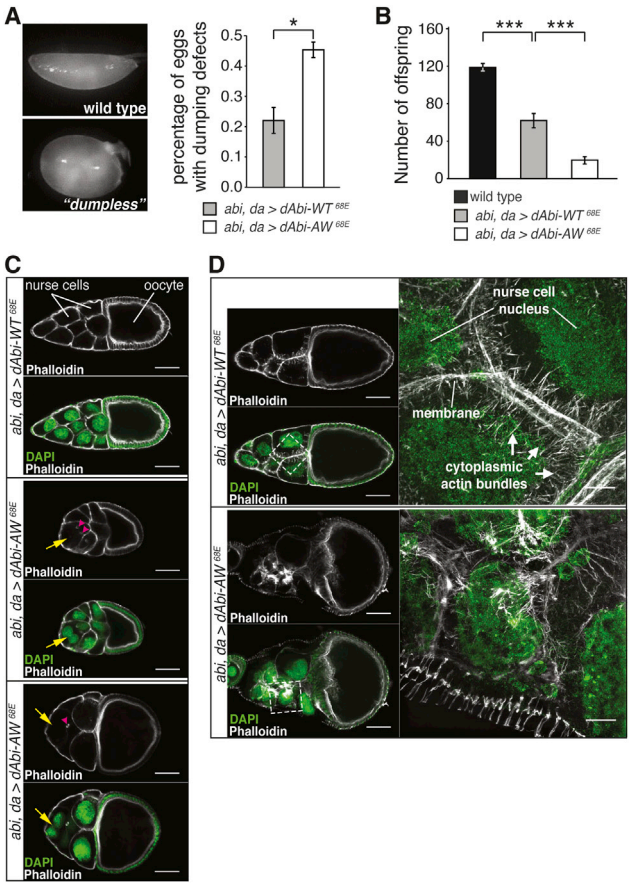

Figure 7. WIRS/WRC Interaction Regulates Oogenesis in Flies

(A) Left, representative images of *Drosophila* WT eggs (top) and eggs with a "dumpless" phenotype. Right, quantification of dumping defects in eggs from flies rescued by either dAbi-WT (n = 3) or dAbi-AW (n = 3). For each genotype, each repeat (n) used ~220 eggs on average dissected from 7–10 female flies.

(B) Quantification of female fertility. Histogram depicts the number of offspring counted from two females mated to WT males. Bars represent offspring per cross (n = 25 crosses).

(C) Representative confocal images of stage 10A egg chambers stained with phalloidin and DAPI. Genotypes as indicated (scale bars, 50 μm). Yellow arrow, lost cortical actin in nurse cells. Magenta arrowhead, ring canals detached from membranes.

(D) Left, representative confocal images of stage 10B egg chambers stained with phalloidin and DAPI. Genotypes as indicated (scale bars, 50 μm). Right, SIM images of regions in the white boxes (scale bars, 10 μm).

Error bars represent SEM; p values were calculated by Student's t test (*p < 0.05 and ***p < 0.0005).

See also Figure S4.

anomalies during late stages of oogenesis (Figure 7C). First, the majority of the dAbi-AW rescued egg chambers were smaller and aberrantly shaped, a phenotype characteristic of defects in "dumping" (Figure 7C, middle) (Hudson and Cooley, 2002b). Occasionally, we also observed an opposite phenotype represented by spherical but larger egg chambers (Figure 7C, bottom); this phenotype was similarly found for *kugelei* (*kug*, *fat2*) female sterile mutants, suggestive of defects in egg chamber elongation rather than in "dumping" (Gutzeit et al., 1991; Viktorinová et al., 2009). Second, independent of the egg chamber size, the cortical actin cytoskeleton in nurse cells was substantially reduced, resulting in formation of multinucleated nurse cells (Figure 7C, yellow arrows). Free-floating ring canals are often observed in such nurse cells as previously observed for *wave* mutants (Figure 7C, magenta arrowheads) (Zallen et al., 2002). Finally, we observed even more severe defects in the actin cytoskeleton in older stages (stage 10B) when actin-myosin-mediated contraction drives the dumping of the remaining cytoplasmic contents from the nurse cells into the oocyte. High-resolution structured illumination microscopy (SIM) revealed that the actin bundles were properly organized in majority of the dAbi-WT rescued egg chambers at stage 10B but were severely disorganized in dAbi-AW rescued egg chambers (Figure 7D), likely due to the aforementioned defects in the cortical actin cytoskeleton. Thus, we propose that the WIRS/WRC interaction may regulate actin cytoskeletal organization during oogenesis and that disrupting the WIRS interaction site of the WRC results in defective egg morphology and female sterility.

The general importance of the WIRS/WRC interaction in biology is further supported by our additional observation that

mutating the WIRS binding site of the WRC also impaired development of the *Drosophila* optic lobe (Figure S4). In this system, the WRC functions non-cell autonomously to regulate photoreceptor neuron axon targeting (Stephan et al., 2011). Taken together, our data suggest that the WIRS/WRC interaction could have diverse and essential functions throughout development.

DISCUSSION

We have identified a consensus peptide motif, WIRS, that specifically binds to a unique surface formed by the Sra and Abi subunits of the WRC. Strict conservation of the binding surface suggests that this interaction is broadly important to metazoans. The WIRS motif defines a novel class of WRC ligands that contains ~120 diverse membrane proteins. Our genetic data further show that mutating the WIRS binding site of the WRC in *Drosophila* disrupts actin cytoskeleton organization and egg morphology during oogenesis, leading to female sterility, and also disrupts development of the visual system. In summary, our data characterize a widespread and conserved interaction that may link numerous membrane proteins to the WRC and the actin cytoskeleton.

Molecular Implications of the WIRS/WRC Interaction

The WIRS binding surface is contributed by both the Sra and Abi subunits of the WRC and therefore is only present in the fully assembled complex. Consequently, the WIRS interaction is unique to the intact WRC and cannot occur with individual subunits or subcomplexes. This may have important functional implications because, in cells, individual WRC subunits may form complexes with other proteins. For example, Sra1 binds the fragile-X mental retardation syndrome protein FMRP, along with the translation initiation factor eIF4E, using an interaction surface that is normally buried within the WRC (Chen et al., 2010; Napoli et al., 2008). Moreover, Abi has been shown to interact with other proteins independent of its assembly into the WRC, including another member of the Wiskott-Aldrich syndrome protein WASP and the Diaphanous-related formin (Bogdan et al., 2005; Ryu et al., 2009). Finally, the Nap1 ortholog Hem1 was suggested to exist in large complexes distinct from the WRC (Weiner et al., 2006). These various complexes likely have distinct cellular functions. For example, the Sra1-FMRP-eIF4E complex regulates mRNA localization and protein translation, and the Abi complexes were shown to regulate the actin cytoskeleton in processes distinct from those regulated by the WRC (Bogdan et al., 2005; Napoli et al., 2008). Therefore, the multisubunit nature of the WIRS binding site may provide a mechanism to specifically regulate the intact WRC.

WIRS proteins can directly recruit the WRC to membranes (Figures 6C and 6D), likely in cooperation with the other classes of WRC ligands. WIRS proteins may also have additional effects on the biochemical activity of the WRC. For example, we have demonstrated that, although the minimal WIRS motif does not activate the WRC, sequences flanking the motif can potentiate (as in PCDH10) or inhibit (as in PCDH17) activity of the WRC in vitro (Figure 5). Therefore, WIRS proteins may exert different effects on the activity of the assembly, again likely in cooperation with other WRC ligands such as Rac1 or kinases. Alternatively, WIRS proteins could act as a scaffold and modulate WRC activity by coordinately recruiting the complex and other ligands. For example, the cytoplasmic tail of the NMDA receptor subunit NR2B could potentially corecruit cyclin-dependent kinase 5 (Cdk5) (Hawasli et al., 2007) and the WRC to facilitate phosphorylation and consequent activation of WAVE (Kim et al., 2006). In fact, many WIRS-containing proteins are thought to function as scaffolds, including APC, Ankyrin, WTX/Amer1, Shroom, and Shank. Finally, many WIRS proteins are cell-cell adhesion receptors, which are often densely clustered at the plasma membrane (Hartman and Groves, 2011). Such clustering would locally concentrate the WRC, a process known to increase the activity of WASP proteins toward the Arp2/3 complex (Padrick et al., 2008; Padrick and Rosen, 2010).

Finally, WIRS/WRC interactions themselves are likely regulated. In fact, our data suggest that the WIRS motif (Φ-x-T/S-F-X-X) could be modulated by phosphorylation. High-affinity binding requires Thr or Ser at the third position of the WIRS motif. No other residues examined are tolerated (Figure 1E). Thus, it is likely that Thr/Ser phosphorylation at this position would block binding as well. Indeed, phosphorylation of various WIRS sites has been identified not only in global phosphoproteome studies but also by site-specific mutagenesis (Hornbeck et al., 2012) (Table S2). Together, these various mechanisms could bring a large range of regulatory dynamics to locally tune WRC activity and consequent actin assembly in vivo.

Evolutionary Implications of the WIRS/WRC Interaction

The conservation of the WIRS binding surface in virtually all metazoans suggests that the WIRS/WRC interaction is broadly important and unique to animals because it is absent from other eukaryotes, including protists, fungi, and plants. It is notable that the WIRS binding surface is found even in nonmetazoan choanoflagellates, suggesting that WIRS/WRC interactions appeared more than 700 million years ago in an early ancestor that predates metazoans. Choanoflagellates are considered to be the closest living relatives to metazoans because they encode many metazoan-specific protein domains, including various cell adhesion molecules and proteins enriched in the nervous system (Burkhardt et al., 2011; King et al., 2008). Although choanoflagellates are generally considered unicellular organisms, they can form simple colonies (Alegado et al., 2012), leading to the possibility that the WIRS interaction arose to maintain multicellularity. However, this interaction may not be strictly necessary for multicellularity, as the WIRS binding surface is not found in the placozoan *T. adhaerens*, a primitive, amoeboid-like metazoan that lacks tissues or organs but is made up of distinct cell types (Srivastava et al., 2008). Moreover, a significant number of nonadhesion proteins also contain WIRS motifs, indicating that the WIRS interaction likely developed additional functions.

In this study, we have limited our search to proteins whose WIRS motifs were conserved in four of seven representative species. Among the ~120 WIRS proteins, some display high conservation of their WIRS motifs. These include netrin receptors and ROBO proteins, whose WIRS motifs are conserved from human to *C. elegans*, despite a significant divergence in

the overall sequences of their cytoplasmic tails. The WIRS motifs of many other proteins, including protocadherins and neuroligins, are conserved in all vertebrates examined (from human to zebrafish). We note that, by using conservation as a criterion in our search, we may have missed other bona fide WIRS ligands that are less conserved.

Physiologic Implications of the WIRS/WRC Interaction

We have demonstrated biological functions of WIRS/WRC interactions in animals by using *Drosophila* oogenesis as a model system. Defects observed by disrupting the WIRS binding surface, which resulted in defective egg morphology, disrupted actin cytoskeleton, and female sterility, resemble defects that arise from knocking out the WRC (Hudson and Cooley, 2002a; Zallen et al., 2002; Zobel and Bogdan, 2013), suggesting that the WIRS interaction plays a major role in regulating WRC function during oogenesis in flies. Additionally, we observed that the WIRS binding site is also important to the WRC in its non-cell-autonomous function of regulating photoreceptor axonal targeting in developing optic lobes (Figure S4) (Stephan et al., 2011). We believe that many more WIRS-mediated regulatory functions are yet to be discovered. In support of this assertion, Shen and colleagues have recently shown that, in *C. elegans*, WIRS-mediated interaction of the neuronal adhesion receptor SYG-1 with the WRC regulates actin assembly at presynaptic sites in the neuromuscular junction of the egg-laying motor neuron HSN and consequently is critical in initiating both synaptogenesis and axonal branching (Chia et al. 2014 [this issue of *Cell*]). We propose that WIRS/WRC interactions are of general and diverse importance to animals throughout development.

Future studies are needed to reveal which specific WIRS-containing ligands are important to particular processes. Prior data in the literature suggest candidate WIRS proteins during oogenesis. Two membrane-associated proteins, P08630 (Tec29 tyrosine kinase) and Q9VCX1 (locomotion defects protein, Loco), both contain WIRS motifs and have been shown to regulate nurse cell dumping (Pathirana et al., 2001; Roulier et al., 1998). Loco was also found to regulate the cortical actin cytoskeleton in glia (Schwabe et al., 2005). Our phenotypic analysis also reveals an opposite oogenesis defect, which is similar to those observed in *kugelei* mutants deficient for dFAT2, another WIRS-containing protein (Gutzeit et al., 1991; Viktorinová et al., 2009). It remains to be determined whether these proteins or others are directly linked to the WRC during this process.

A variety of evidence also exists in the literature, suggesting functional roles of the WIRS interaction in other biological processes. In addition to PCDH10 and PCDH19, the WIRS proteins DCC and ROBO and the epithelial sodium channel ENaC (γ subunit) have been genetically linked to the WRC. DCC and ROBO differentially regulate the abundance and subcellular localization of the WRC to control the actin cytoskeleton in *C. elegans* embryonic epidermis (Bernadskaya et al., 2012). The WRC and Rac1 were found to be essential in regulating the activity of ENaC (Karpushev et al., 2011). Our data suggest that these genetic interactions may be due to direct physical interactions of WIRS motifs with the WRC. The functions of many other WIRS proteins, only a few of which have been previously linked to the actin cytoskeleton (e.g., glutamate receptor NR2B and the postsynaptic cell adhesion molecule Neuroligin1), may also depend on an interaction with the WRC. As a notable example, a 21 amino acid sequence of the Neuroligin1 cytoplasmic tail harboring a WIRS motif (PGIQPLHT FNTFTGGQNNTLP, WIRS underlined) is required for presynaptic terminal maturation (Wittenmayer et al., 2009).

Although it is still very premature to link WIRS/WRC interactions to any disease, several cases are suggestive (Table S2). For example, seven cases of epilepsy and mental retardation in females (EFMR) were reported to arise from truncations of the cytoplasmic tail of PCDH19, all resulting in the loss of its WIRS motif (Dimova et al., 2012). Additionally, partial truncation of the DCC cytoplasmic tail, along with its WIRS motif, caused congenital mirror movement in four affected members of a three generation Italian family (Depienne et al., 2011). Finally, a point mutation (S1359C) that disrupts the WIRS site (LDSFES, S1359 underlined) in the adenomatous polyposis coli (APC) protein was associated with three unrelated cases of hepatoblastoma (Oda et al., 1996).

Conclusions

In summary, we have defined and characterized a large family of potential WRC ligands unique to metazoans. A large and diverse set of membrane proteins comprises this class, many with important biological functions. Our findings provide a mechanistic framework to understand how these proteins signal downstream to the actin cytoskeleton via direct interaction with the WRC and how their mutations may ultimately lead to disease.

EXPERIMENTAL PROCEDURES

DNA constructs and peptides used in this study are listed in the Extended Experimental Procedures (Table S3).

Protein Purification

Recombinant WRCs were generated as previously described (Chen et al., 2010; Ismail et al., 2009). GST-tagged cytoplasmic tails of different transmembrane receptors were purified by glutathione affinity chromatography or followed by ion exchange and size exclusion chromatographies.

Crystallography

Crystals of WIRS/miniWRC complex were grown under similar conditions as was the apo miniWRC (Chen et al., 2010) except that the hanging drops also contained ~2.6 mM seleno-WIRS peptide. The structure was solved by molecular replacement from the structure of the apo miniWRC, using the program suite PHENIX (Adams et al., 2010) and Coot (Emsley et al., 2010). Final coordinates are available from the RCSB with accession code rcsb082839 (PDB ID 4N78).

Biochemical Assays

GST or MBP pull down was performed by mixing bait proteins and 5- to 10-fold excess of prey proteins with the corresponding affinity beads. After incubation and washing, the bound proteins were eluted with reduced glutathione or maltose, respectively. Pyrene-actin assembly assays were performed as previously described (Ismail et al., 2009). Coimmunoprecipitation was performed by mixing mouse brain lysate with anti-WAVE1 monoclonal antibody (Sigma) and protein A/G beads in the presence of different competitors. The bound proteins were eluted by incubation with peptide A (Table S3) and analyzed by SDS PAGE followed by western blotting.

Cellular Assays

The bead clustering experiment was performed using NIH 3T3 cells stably expressing Sra1-YPet and transiently transfected with CD16-CD7-CT-mCherry chimeric receptors (Kolanus et al., 1993). Receptors were clustered using an anti-CD16 monoclonal mouse antibody (Invitrogen) followed by Dynal beads coated with sheep-anti-mouse IgG (Invitrogen). Fixed cells were imaged using confocal microscopy along z stacks to find the beads with enriched mCherry signals and were blind scored for enriched Ypet signals.

Drosophila Genetics and Immunohistochemistry

Transgenic flies were prepared as previously described (Stephan et al., 2011). UASt-dAbi^{68E} and UASp-dAbi^{68E} wild-type and mutant transgenes were generated by ΦC31-integrase-mediated integration into the landing site M{3xP3-RFP.attP'}ZH-68E (Bischof et al., 2007). The *abi* inserts were sequenced and cloned into pUASTattB rfA and pUASPattB rfA (*Drosophila* Genomics Resource Center, DGRC), respectively, by LR in vitro recombination (Invitrogen). Brains of third instar larvae were dissected, stained as previously described (Stephan et al., 2011), and blind scored after 3D reconstruction of confocal fluorescent images. Egg chambers from dissected ovaries were stained and imaged as previously described (Bogdan et al., 2005). In fertility assays, two females of each genotype were mated with three wild-type males. The number of offspring was counted after 15 days.

Identification of WIRS Proteins

The annotated Swiss-Prot database (Lane et al., 2012) was searched for human sequences containing the consensus WIRS motif ([FMWYIL]-x-[TS]-[F]). The identified sequences were filtered to retain those whose WIRS (1) was cytoplasmic and (2) resided in disordered regions. Proteins with WIRS motifs existing in less than four representative animal species (human, mouse, chicken, frog, zebrafish, *Drosophila*, and *C. elegans*) were finally removed.

SUPPLEMENTAL INFORMATION

Supplemental Information includes Extended Experimental Procedures, four figures, and three tables and can be found with this article online at http://dx.doi.org/10.1016/j.cell.2013.11.048.

AUTHOR CONTRIBUTIONS

Co-second authors Z.C., K.B., and C.W.P. contributed equally to this work and are listed in alphabetical order in the author list. M.K.R. oversaw biochemical, structural, and cell biological work. S.B. oversaw fly work. B.C., C.W.P. and M.K.R. conceived of the project. B.C. performed all biochemical experiments. Z.C. determined the structure of the WRC/WIRS complex. B.C., Z.C., and M.K.R. analyzed the structure. K.B. and S.B. performed fly genetics experiments. C.W.P. performed the cellular experiments. Y.L. and S.S. performed bioinformatic analyses with advice from N.V.G. L.H. maintained insect cell culture. B.C., C.P., and M.K.R. wrote the manuscript with assistance from all authors.

ACKNOWLEDGMENTS

We thank K. Roybal and C. Wuelfing for making MMLVs for generating stable Sra1-YPet cell lines; S.B. Padrick for help in fitting the anisotropy data; S.B. Padrick, K. Huber, and P. Li for discussion; B.T. Nixon, Y.M. Chook, S.B. Padrick, D. Jia, T. Zobel, J. Squarr, and M. Bechtold for reviewing the manuscript; and N. Brose, I. Bezprozvanny, T.C. Südhof, K. Huber, K.W. Roche, J.R. Bamburg, and T. Pawson for sharing the vectors for hNeuroligin-4X, rCav1.3, hBAI3, rmGluR5, rGluR6, mCherry, and hCD16-hCD7, respectively. Research was supported by fellowships from the American Heart Association, the Cancer Research Institute, and the National Institutes of Health (NIH) (1F32DK091074) to B.C., Z.C., and C.W.P., respectively, grants to S.B. from the Deutsche Forschungsgemeinschaft (DFG), grants from the NIH and Welch Foundation to M.K.R. (R01-GM056322 and I-1544, respectively) and N.V.G. (R01-GM094575 and I-1550, respectively), and the Howard Hughes Medical Institute. Use of the Argonne National Laboratory Structural Biology Center beamlines at the Advanced Photon Source was supported by the U.S. Department of Energy under contract DE-AC02-06CH11357.

Received: January 22, 2013
Revised: September 6, 2013
Accepted: November 25, 2013
Published: January 16, 2014

REFERENCES

Adams, P.D., Afonine, P.V., Bunkóczi, G., Chen, V.B., Davis, I.W., Echols, N., Headd, J.J., Hung, L.W., Kapral, G.J., Grosse-Kunstleve, R.W., et al. (2010). PHENIX: a comprehensive Python-based system for macromolecular structure solution. Acta Crystallogr. D Biol. Crystallogr. *66*, 213–221.

Alegado, R.A., Brown, L.W., Cao, S., Dermenjian, R.K., Zuzow, R., Fairclough, S.R., Clardy, J., and King, N. (2012). A bacterial sulfonolipid triggers multicellular development in the closest living relatives of animals. Elife *1*, e00013.

Ashkenazy, H., Erez, E., Martz, E., Pupko, T., and Ben-Tal, N. (2010). ConSurf 2010: calculating evolutionary conservation in sequence and structure of proteins and nucleic acids. Nucleic Acids Res. *38* (Web Server issue), W529–W533.

Bastock, R., and St Johnston, D. (2008). Drosophila oogenesis. Curr. Biol. *18*, R1082–R1087.

Bernadskaya, Y.Y., Wallace, A., Nguyen, J., Mohler, W.A., and Soto, M.C. (2012). UNC-40/DCC, SAX-3/Robo, and VAB-1/Eph polarize F-actin during embryonic morphogenesis by regulating the WAVE/SCAR actin nucleation complex. PLoS Genet. *8*, e1002863.

Bilder, D., and Haigo, S.L. (2012). Expanding the morphogenetic repertoire: perspectives from the Drosophila egg. Dev. Cell *22*, 12–23.

Bischof, J., Maeda, R.K., Hediger, M., Karch, F., and Basler, K. (2007). An optimized transgenesis system for Drosophila using germ-line-specific phiC31 integrases. Proc. Natl. Acad. Sci. USA *104*, 3312–3317.

Bogdan, S., Stephan, R., Löbke, C., Mertens, A., and Klämbt, C. (2005). Abi activates WASP to promote sensory organ development. Nat. Cell Biol. *7*, 977–984.

Buck, M., Xu, W., and Rosen, M.K. (2004). A two-state allosteric model for autoinhibition rationalizes WASP signal integration and targeting. J. Mol. Biol. *338*, 271–285.

Burkhardt, P., Stegmann, C.M., Cooper, B., Kloepper, T.H., Imig, C., Varoqueaux, F., Wahl, M.C., and Fasshauer, D. (2011). Primordial neurosecretory apparatus identified in the choanoflagellate Monosiga brevicollis. Proc. Natl. Acad. Sci. USA *108*, 15264–15269.

Campellone, K.G., and Welch, M.D. (2010). A nucleator arms race: cellular control of actin assembly. Nat. Rev. Mol. Cell Biol. *11*, 237–251.

Chia, P.-H., Chen, B., Li, P., Rosen, M.K., and Shen, K. (2014). Local F-actin network links synapse formation and axon branching. Cell *156*, this issue, 208–220.

Chen, Z., Borek, D., Padrick, S.B., Gomez, T.S., Metlagel, Z., Ismail, A.M., Umetani, J., Billadeau, D.D., Otwinowski, Z., and Rosen, M.K. (2010). Structure and control of the actin regulatory WAVE complex. Nature *468*, 533–538.

Depienne, C., Cincotta, M., Billot, S., Bouteiller, D., Groppa, S., Brochard, V., Flamand, C., Hubsch, C., Meunier, S., Giovannelli, F., et al. (2011). A novel DCC mutation and genetic heterogeneity in congenital mirror movements. Neurology *76*, 260–264.

Dibbens, L.M., Tarpey, P.S., Hynes, K., Bayly, M.A., Scheffer, I.E., Smith, R., Bomar, J., Sutton, E., Vandeleur, L., Shoubridge, C., et al. (2008). X-linked protocadherin 19 mutations cause female-limited epilepsy and cognitive impairment. Nat. Genet. *40*, 776–781.

Dimova, P.S., Kirov, A., Todorova, A., Todorov, T., and Mitev, V. (2012). A novel PCDH19 mutation inherited from an unaffected mother. Pediatr. Neurol. *46*, 397–400.

Eden, S., Rohatgi, R., Podtelejnikov, A.V., Mann, M., and Kirschner, M.W. (2002). Mechanism of regulation of WAVE1-induced actin nucleation by Rac1 and Nck. Nature *418*, 790–793.

Emond, M.R., Biswas, S., and Jontes, J.D. (2009). Protocadherin-19 is essential for early steps in brain morphogenesis. Dev. Biol. *334*, 72–83.

Emsley, P., Lohkamp, B., Scott, W.G., and Cowtan, K. (2010). Features and development of Coot. Acta Crystallogr. D Biol. Crystallogr. *66*, 486–501.

Gutzeit, H.O., Eberhardt, W., and Gratwohl, E. (1991). Laminin and basement membrane-associated microfilaments in wild-type and mutant Drosophila ovarian follicles. J. Cell Sci. *100*, 781–788.

Hartman, N.C., and Groves, J.T. (2011). Signaling clusters in the cell membrane. Curr. Opin. Cell Biol. *23*, 370–376.

Hawasli, A.H., Benavides, D.R., Nguyen, C., Kansy, J.W., Hayashi, K., Chambon, P., Greengard, P., Powell, C.M., Cooper, D.C., and Bibb, J.A. (2007). Cyclin-dependent kinase 5 governs learning and synaptic plasticity via control of NMDAR degradation. Nat. Neurosci. *10*, 880–886.

Ho, H.Y., Rohatgi, R., Lebensohn, A.M., Le Ma, Li, J., Gygi, S.P., and Kirschner, M.W. (2004). Toca-1 mediates Cdc42-dependent actin nucleation by activating the N-WASP-WIP complex. Cell *118*, 203–216.

Hornbeck, P.V., Kornhauser, J.M., Tkachev, S., Zhang, B., Skrzypek, E., Murray, B., Latham, V., and Sullivan, M. (2012). PhosphoSitePlus: a comprehensive resource for investigating the structure and function of experimentally determined post-translational modifications in man and mouse. Nucleic Acids Res. *40* (Database issue), D261–D270.

Hudson, A.M., and Cooley, L. (2002a). A subset of dynamic actin rearrangements in Drosophila requires the Arp2/3 complex. J. Cell Biol. *156*, 677–687.

Hudson, A.M., and Cooley, L. (2002b). Understanding the function of actin-binding proteins through genetic analysis of Drosophila oogenesis. Annu. Rev. Genet. *36*, 455–488.

Ismail, A.M., Padrick, S.B., Chen, B., Umetani, J., and Rosen, M.K. (2009). The WAVE regulatory complex is inhibited. Nat. Struct. Mol. Biol. *16*, 561–563.

Karpushev, A.V., Levchenko, V., Ilatovskaya, D.V., Pavlov, T.S., and Staruschenko, A. (2011). Novel role of Rac1/WAVE signaling mechanism in regulation of the epithelial Na+ channel. Hypertension *57*, 996–1002.

Kim, Y., Sung, J.Y., Ceglia, I., Lee, K.W., Ahn, J.H., Halford, J.M., Kim, A.M., Kwak, S.P., Park, J.B., Ho Ryu, S., et al. (2006). Phosphorylation of WAVE1 regulates actin polymerization and dendritic spine morphology. Nature *442*, 814–817.

King, N., Westbrook, M.J., Young, S.L., Kuo, A., Abedin, M., Chapman, J., Fairclough, S., Hellsten, U., Isogai, Y., Letunic, I., et al. (2008). The genome of the choanoflagellate Monosiga brevicollis and the origin of metazoans. Nature *451*, 783–788.

Kolanus, W., Romeo, C., and Seed, B. (1993). T cell activation by clustered tyrosine kinases. Cell *74*, 171–183.

Koronakis, V., Hume, P.J., Humphreys, D., Liu, T., Hørning, O., Jensen, O.N., and McGhie, E.J. (2011). WAVE regulatory complex activation by cooperating GTPases Arf and Rac1. Proc. Natl. Acad. Sci. USA *108*, 14449–14454.

Lane, L., Argoud-Puy, G., Britan, A., Cusin, I., Duek, P.D., Evalet, O., Gateau, A., Gaudet, P., Gleizes, A., Masselot, A., et al. (2012). neXtProt: a knowledge platform for human proteins. Nucleic Acids Res. *40* (Database issue), D76–D83.

Lebensohn, A.M., and Kirschner, M.W. (2009). Activation of the WAVE complex by coincident signals controls actin assembly. Mol. Cell *36*, 512–524.

Morrow, E.M., Yoo, S.Y., Flavell, S.W., Kim, T.K., Lin, Y., Hill, R.S., Mukaddes, N.M., Balkhy, S., Gascon, G., Hashmi, A., et al. (2008). Identifying autism loci and genes by tracing recent shared ancestry. Science *321*, 218–223.

Nakao, S., Platek, A., Hirano, S., and Takeichi, M. (2008). Contact-dependent promotion of cell migration by the OL-protocadherin-Nap1 interaction. J. Cell Biol. *182*, 395–410.

Napoli, I., Mercaldo, V., Boyl, P.P., Eleuteri, B., Zalfa, F., De Rubeis, S., Di Marino, D., Mohr, E., Massimi, M., Falconi, M., et al. (2008). The fragile X syndrome protein represses activity-dependent translation through CYFIP1, a new 4E-BP. Cell *134*, 1042–1054.

Oda, H., Imai, Y., Nakatsuru, Y., Hata, J., and Ishikawa, T. (1996). Somatic mutations of the APC gene in sporadic hepatoblastomas. Cancer Res. *56*, 3320–3323.

Oikawa, T., Yamaguchi, H., Itoh, T., Kato, M., Ijuin, T., Yamazaki, D., Suetsugu, S., and Takenawa, T. (2004). PtdIns(3,4,5)P3 binding is necessary for WAVE2-induced formation of lamellipodia. Nat. Cell Biol. *6*, 420–426.

Padrick, S.B., and Rosen, M.K. (2010). Physical mechanisms of signal integration by WASP family proteins. Annu. Rev. Biochem. *79*, 707–735.

Padrick, S.B., Cheng, H.C., Ismail, A.M., Panchal, S.C., Doolittle, L.K., Kim, S., Skehan, B.M., Umetani, J., Brautigam, C.A., Leong, J.M., and Rosen, M.K. (2008). Hierarchical regulation of WASP/WAVE proteins. Mol. Cell *32*, 426–438.

Pathirana, S., Zhao, D., and Bownes, M. (2001). The Drosophila RGS protein Loco is required for dorsal/ventral axis formation of the egg and embryo, and nurse cell dumping. Mech. Dev. *109*, 137–150.

Pollitt, A.Y., and Insall, R.H. (2009). WASP and SCAR/WAVE proteins: the drivers of actin assembly. J. Cell Sci. *122*, 2575–2578.

Rørth, P. (1998). Gal4 in the Drosophila female germline. Mech. Dev. *78*, 113–118.

Roulier, E.M., Panzer, S., and Beckendorf, S.K. (1998). The Tec29 tyrosine kinase is required during Drosophila embryogenesis and interacts with Src64 in ring canal development. Mol. Cell *1*, 819–829.

Ryu, J.R., Echarri, A., Li, R., and Pendergast, A.M. (2009). Regulation of cell-cell adhesion by Abi/Diaphanous complexes. Mol. Cell. Biol. *29*, 1735–1748.

Schwabe, T., Bainton, R.J., Fetter, R.D., Heberlein, U., and Gaul, U. (2005). GPCR signaling is required for blood-brain barrier formation in drosophila. Cell *123*, 133–144.

Srivastava, M., Begovic, E., Chapman, J., Putnam, N.H., Hellsten, U., Kawashima, T., Kuo, A., Mitros, T., Salamov, A., Carpenter, M.L., et al. (2008). The Trichoplax genome and the nature of placozoans. Nature *454*, 955–960.

Stavoe, A.K., Nelson, J.C., Martínez-Velázquez, L.A., Klein, M., Samuel, A.D., and Colón-Ramos, D.A. (2012). Synaptic vesicle clustering requires a distinct MIG-10/Lamellipodin isoform and ABI-1 downstream from Netrin. Genes Dev. *26*, 2206–2221.

Stephan, R., Gohl, C., Fleige, A., Klämbt, C., and Bogdan, S. (2011). Membrane-targeted WAVE mediates photoreceptor axon targeting in the absence of the WAVE complex in Drosophila. Mol. Biol. Cell *22*, 4079–4092.

Suetsugu, S., Kurisu, S., Oikawa, T., Yamazaki, D., Oda, A., and Takenawa, T. (2006). Optimization of WAVE2 complex-induced actin polymerization by membrane-bound IRSp53, PIP(3), and Rac. J. Cell Biol. *173*, 571–585.

Tai, K., Kubota, M., Shiono, K., Tokutsu, H., and Suzuki, S.T. (2010). Adhesion properties and retinofugal expression of chicken protocadherin-19. Brain Res. *1344*, 13–24.

Takenawa, T., and Suetsugu, S. (2007). The WASP-WAVE protein network: connecting the membrane to the cytoskeleton. Nat. Rev. Mol. Cell Biol. *8*, 37–48.

Uemura, M., Nakao, S., Suzuki, S.T., Takeichi, M., and Hirano, S. (2007). OL-Protocadherin is essential for growth of striatal axons and thalamocortical projections. Nat. Neurosci. *10*, 1151–1159.

Viktorinová, I., König, T., Schlichting, K., and Dahmann, C. (2009). The cadherin Fat2 is required for planar cell polarity in the Drosophila ovary. Development *136*, 4123–4132.

Weiner, O.D., Rentel, M.C., Ott, A., Brown, G.E., Jedrychowski, M., Yaffe, M.B., Gygi, S.P., Cantley, L.C., Bourne, H.R., and Kirschner, M.W. (2006). Hem-1 complexes are essential for Rac activation, actin polymerization, and myosin regulation during neutrophil chemotaxis. PLoS Biol. *4*, e38.

Wittenmayer, N., Körber, C., Liu, H., Kremer, T., Varoqueaux, F., Chapman, E.R., Brose, N., Kuner, T., and Dresbach, T. (2009). Postsynaptic Neuroligin1 regulates presynaptic maturation. Proc. Natl. Acad. Sci. USA *106*, 13564–13569.

Ying, J., Li, H., Seng, T.J., Langford, C., Srivastava, G., Tsao, S.W., Putti, T., Murray, P., Chan, A.T., and Tao, Q. (2006). Functional epigenetics identifies a protocadherin PCDH10 as a candidate tumor suppressor for nasopharyngeal, esophageal and multiple other carcinomas with frequent methylation. Oncogene *25*, 1070–1080.

Zallen, J.A., Cohen, Y., Hudson, A.M., Cooley, L., Wieschaus, E., and Schejter, E.D. (2002). SCAR is a primary regulator of Arp2/3-dependent morphological events in Drosophila. J. Cell Biol. *156*, 689–701.

Zobel, T., and Bogdan, S. (2013). A high resolution view of the fly actin cytoskeleton lacking a functional WAVE complex. J. Microsc. *251*, 224–231.